



Water use of a super high-density olive orchard submitted to regulated deficit irrigation in Mediterranean environment over three contrasted years

Rossana Monica Ferrara¹ · Maria Roberta Bruno¹ · Pasquale Campi¹ · Salvatore Camposeo² · Gabriele De Carolis¹ · Liliana Gaeta¹ · Nicola Martinelli¹ · Marcello Mastrorilli¹ · Anna Francesca Modugno¹ · Teresa Mongelli¹ · Mariagrazia Piarulli¹ · Sergio Ruggieri¹ · Gianfranco Rana¹

Received: 12 May 2023 / Accepted: 9 October 2023 / Published online: 31 October 2023
© The Author(s), under exclusive licence to Springer-Verlag GmbH Germany, part of Springer Nature 2023

Abstract

The measurement of transpiration at the field level is a challenging topic in crop water use research, particularly for orchards. The super high-density olive orchard system is in great expansion all over the world, so these investigations are necessary to assess the trees water use under different irrigation techniques. Here, transpiration at plant and stand scales was measured using the sap flow thermal dissipation method, in an olive orchard (cv. “*Arbosana*”) subjected to standard (SI) and regulated deficit irrigation (RDI) with a withholding irrigation period under Mediterranean climate (southern Italy). The measurement method was used after specific calibration and correction for wound effect, azimuthal and gradient errors. Water use efficiency (WUE) and water productivity were determined over three complete growth seasons (2019–2022). The seasons were submitted to highly contrasted weathers. Measurements of stem water potential and stomatal conductance showed that the RDI trees were under mild-moderate water stress only during the withholding irrigation period, otherwise the two treatments were under the same good water conditions. Following these small water differences between treatments, results showed that seasonal transpiration (E_p) was not significantly different in the two treatments in all seasons (249 and 267 mm, 249 and 262 mm, 231 and 202 mm for SI and RDI in the three seasons, respectively) and that WUE was greater in RDI treatment without any impact on yield. The main conclusion is that, when the available water in the soil is limited, olive trees decrease transpiration under any atmospheric conditions, but when the water in the soil is amply available, high atmospheric demand conditions lead to a decrease in tree transpiration.

Introduction

The increasing instabilities of precipitation regimes coupled with the steady increase of air temperature due to global warming impose crop adaptation strategies to climate change. Irrigation is a common adaptation agricultural technique, even for crops traditionally grown under rainfed conditions, hence, studies to quantify water requirements and to understand crop water use must be updated. One such crop is

Olea europaea L. var. *sativa* Hoff. et Lk., whose plant water status and water consumption have been an object of several studies in the last decades (i.a., Aganchich et al. 2007; Agüero Alcaras et al. 2016; Fernández et al. 2020), since this fruit tree crop is notably efficient to face drought, being very well adapted to arid and semiarid climates (Tognetti et al. 2009). Olive cultivation is becoming more intensive, with the widespread adoption and the strong increase in the Mediterranean region of the super high density (SHD) cropping systems (Godini et al. 2011; Fraga et al. 2021). These mechanized olive groves are characterised by a density of over 1200 trees per hectare cultivated in regular rows (hedgerow orchards). Irrigated SHD orchards show a positive environmental impact compared to rainfed traditional olive orchards, both in terms of carbon and water footprint (Pellegrini et al. 2016; Camposeo et al. 2022). Nevertheless, the eco-physiological responses of olive cultivars to water supply are still poorly or not investigated for complete crop

✉ Gianfranco Rana
gianfranco.rana@crea.gov.it

¹ Council for Agricultural Research and Economics, Agriculture and Environment Research Centre (CREA-AA), Bari, Italy

² Department of Agricultural and Environmental Sciences, University of Bari Aldo Moro, Bari, Italy

seasons (Chebbi et al. 2018), mainly when, in adult orchards, rejuvenation pruning is carried out to restore both trees bearing function and sizes suitable for continuous harvesting machines (Vivaldi et al. 2015; Albarracín et al. 2018).

The Mediterranean region is known to be strongly negatively affected by increases in air temperature and changes in seasonal rainfall distribution (Giorgi 2006; Espadafor et al. 2011; Rana et al. 2016; Katerji et al. 2017). In this important agricultural area, among the different proposed strategies to reduce freshwater use for SHD olive orchards, several studies demonstrated that the regulated deficit irrigation (RDI) can be a suitable strategy for reducing the excessive vigour of the species, through limiting the soil water availability (Iniesta et al. 2009; Fernández et al. 2013; Rosecrance et al. 2015). Iniesta et al. (2009) and Fernández et al. (2020) indicated that RDI allows to save 60% of irrigation water without significantly compromising the oil production and quality. Aganchich et al. (2007) and Agüero Alcaras et al. (2016) showed that typical Mediterranean olive cultivars under RDI optimized water use by decreasing stomatal conductance, stem water potential and relative water content compared to full irrigation treatment. It has also been extensively demonstrated that in SHD olive orchards the controlled water stress has little effect on oil yield and a positive effect on oil quality (i.a., Tognetti et al. 2006; García et al. 2017). Furthermore, since climate change impacts on crop yield and has also strong effects on soil water budget, water use by the plants and water productivity, it is necessary to update and investigate the adaptability of crops to changing, and often contrasting, growth season weathers (Kang et al. 2009).

The crop water use efficiency (WUE) is defined as the ratio between actual crop evapotranspiration (ET) and the amount of water supplied by irrigation and precipitation (Fernández et al. 2020; Eq. (1) in reported Table 1); from an agronomical perspective the concept of water productivity (WP) is preferable, defined as the ratio between yield and actual transpiration (Bouman 2007; Fernández et al. 2020). The lack of knowledge on the values of water losses by transpiration for entire growing seasons brings to incorrect or inaccurate values of WUE and WP (Katerji et al. 2008; Fernández et al. 2020). To correctly evaluate the WUE or, in general, the WR of a crop, it is necessary to determine with high accuracy the crop water losses (Katerji et al. 2008), particularly complex for orchards (Rana and Katerji 2000; Scanlon and Kustas 2012; Cammalleri

et al. 2013). The micrometeorological methods generally resulted in the best way to measure ET; starting from ET measured by the eddy covariance technique, the transpiration can be determined by partitioning methods (Rana et al. 2018). These approaches can estimate transpiration with a suitable accuracy, but measurements must be carried out above large surfaces (Lee et al. 2004), resulting in difficult application in studies where comparison of treatments are performed. For these latter, methods to measure transpiration at the plant level are preferred, and the most widespread methods to determine it at a single plant scale are based on the measurement of mass flux density (Rana and Katerji 2000). The thermal dissipation method (TDM) (Granier 1985, 1987) has been frequently used to determine the actual transpiration of olive orchards in different situations (Masmoudi et al. 2011; Cammalleri et al. 2013; Agüero Alcaras et al. 2016; Conceição et al. 2017; Kokkotos et al. 2021). However, due to issues related to the TDM technique, the total water losses from transpiration in olive orchards on yearly and/or growth seasonal time scale are almost always unknown or affected by large uncertainties. As a result, olive orchard WUE and WP values are often limited to incomplete or reduced/restricted growth seasons (Burgess et al. 2001; Chebbi et al. 2018).

The general objective of this mid-term study was to analyse the eco-physiological behaviour of olive trees (cv. *Arbosana*) grown in an adult SHD orchard subjected to standard irrigation *versus* regulated deficit irrigation, to evaluate the impact of water deficit on seasonal—yearly WUE and WP, at both plant and canopy scale. Actual transpiration was continuously monitored using TDM, specifically calibrated and corrected, in three complete growing seasons (2019–2020; 2020–2021; 2021–2022, 1096 days in total) including a rejuvenation pruning event, in a Mediterranean area (southern Italy); the experimental period was characterized by highly contrasted weathers, including very dry and very wet seasons. To generalize the agronomic results, relationships between transpiration and water use variables were investigated.

Table 1 Summary of vapour pressure deficit (VPD), air temperature (T), global radiation (R_g) and rain in the three growth seasons

Growth season	VPD (kPa)		T (°C)		R_g (MJ m ⁻² day ⁻¹)		Rain (mm)
	Range	Mean ± SD	Range	Mean ± SD	Range	Mean ± SD	
2019–2020	0.1–2.8	0.8 ± 0.6	0.0–27.7	14.6 ± 7.8	5.6–30.5	17.4 ± 6.3	221
2020–2021	0.0–2.3	0.7 ± 0.5	0.0–30.0	15.6 ± 8.6	2.4–29.1	16.2 ± 6.4	695
2021–2022	0.0–4.1	1.1 ± 0.8	0.0–30.3	18.8 ± 7.9	3.0–34.0	17.0 ± 6.6	288

Materials and methods

The site and the orchard

Measurements were continuously carried out from 1 March 2019 to 28 February 2022 in an olive orchard located at the University of Bari experimental farm in Valenzano, southern Italy (41° 01' N; 16° 45' E; 110 m a.s.l.). The soil is sandy clay (sand, 630 g kg⁻¹; silt, 160 g kg⁻¹; clay, 210 g kg⁻¹) classified as a Typic Haploxeralf (USDA) or Chromi-Cutanic Luvisol (FAO). These textural characteristics do not change with the vertical dimension. At a depth of 0.5 m, a parent rock reduces the capacity of the root systems to expand beyond this layer. The site is characterised by a typical Mediterranean climate with a long-term average (1988–2018) annual rainfall of 560 mm, two third concentrated from autumn to winter, and a long-term average annual temperature of 15.6 °C.

The olive grove was planted in early summer 2006; the self-rooted trees (*cv. Arbosana*) were trained according to the central leader system and spaced 4.0 m × 1.5 m (1667 trees ha⁻¹) with a North–South rows orientation, according to the SHD cropping system. Routine cultural nutrition, soil management, pests and disease control practices were set up as described by Camposeo and Godini (2010). During the experimental period, the olive trees were heavily pruned in March 2020, reducing the canopy volume by 65% (from 5.3 m³ to 2.2 m³ per tree). This rejuvenation pruning was scheduled at the end of the 14th year after planting. However, the recovery of canopy volume was fairly quick: in fact, in the second year after hard pruning (2022) the canopy regrowth was +90% with respect to the pruned trees values (from 2.2 to 4.2 m³ tree⁻¹, see details in Supplementary Material I).

Two plots of 180 m² surface, 60 m apart, with 35 trees in each one, were subjected to two irrigation regimes: the first one followed the standard use of the famers (SI), with a reduction of the full irrigation for improving the oil quality, versus RDI applied throughout the pit hardening phase (Cajias et al. 2016; Hernández et al. 2018; Corell et al. 2022; Ahumada-Orellana et al. 2023) when the tree is least sensitive to water deficit (Goldhamer 1999). During this phenological phase, irrigation was interrupted for about one month per season (19 July–20 August 2019; 15 July–18 August 2020; 14 July–14 August 2021). Irrigation was scheduled according to the ET method, by restoring 86% of actual crop evapotranspiration (ET_c) lost in each irrigation interval. ET_c was calculated using Eq. (1) recommended by the FAO56 guideline as:

$$ET_c = K_r K_c ET_0, \quad (1)$$

where K_r is the reduction coefficient (0.86; Allen and Pereira 2009), K_c ($K_{c_{ini}}=0.5$, $K_{c_{mid}}=0.6$, $K_{c_{end}}=0.5$) is the crop

coefficient, ET_0 is the reference evapotranspiration, calculated by the Penman–Monteith method (Allen et al. 1998). The plots were irrigated by a dripline equipped with 2.5 L h⁻¹ emitters, 0.6 m apart.

For comparing WUE in different years, the beginning of each olive growth season for the WUE and WP calculations was considered to be March 1st because the end of the dormancy period usually falls in January–February, at least for most olive cultivars in the Mediterranean region (Oteros et al. 2013; Aguilera et al. 2014; Fernández 2014). The three growth seasons are: first, 1 March 2019 to 29 February 2020; second, 1 March 2020 to 28 February 2021; third, 1 March 2021 to 28 February 2022.

Weather variables and tree transpiration

Air temperature (T , °C) and vapour pressure deficit (VPD, kPa) through air relative humidity, global radiation (R_g , MJ m⁻² s⁻¹) and precipitation (P , mm) were collected at a standard agrometeorological station 120 m far from the experimental field. To determine the degree of drought for each year under investigation, the standard precipitation index (SPI, Naresh Kumar et al. 2009) was calculated as:

$$SPI = \frac{x_i - x}{s}, \quad (2)$$

with x_i yearly precipitation, x and s long-term average precipitation and standard deviation values, respectively. Value of SPI lower than -1 and higher than 1 indicates dry and wet conditions, respectively.

To determine the atmospheric demand in water terms, the potential evaporation was calculated following Katerji and Rana (2011); in this case E_0 was estimated as:

$$E_0 = \frac{1}{\lambda} \frac{\epsilon r_a A + \rho c_p VPD/\gamma}{(1 + \epsilon)r_a}. \quad (3)$$

Mass flux density, J_i (g m⁻² s⁻¹), was measured in a set of selected plants, by means of TDM (Granier 1985, 1987), by the difference in temperature (ΔT) between two probes (one heated and one unheated) placed in the conducting xylem of the stem. Commercial 20 mm sap flow probes (SFS2 Type M, UP, Steinfurt, Germany) were installed at 0.30–0.40 m above the ground on the north side of each tree. The probes in each sampled tree were covered by a reflecting radiation screen to protect them from rain. ΔT was continuously monitored by two data loggers (CR10X, Campbell Scientific, Utah, USA) which took measurements every 10 s and recorded the average values every 10 min. Details on the TDM measurement procedure are reported in Rana et al. (2020). Measurements were carried out in three replicate trees per irrigation treatment and averaged. Trees have been selected to be representative of each plot, considering the

similar vigour, according to the frequency distribution of trunk diameters and tree size of the whole plot. Time series of daily values of plant transpiration (E_p) were analysed as replications along the growing season. The mass flux density of the selected six trees (three per treatment) was not significantly different ($P < 0.01$) in the first three months of the experiment, before the differentiation of the irrigation regime (Fig. 1), when the mass flux density was, furthermore, not affected by the wound effects.

The application of the TDM method requires specific local species-specific calibration and may be affected by wounds and inhomogeneities in the sapwood, both radially and azimuthally, due to wood anatomy and soil water availability (e.g., Nadezhdina et al. 2007; Fuchs et al. 2017). Therefore, a specific procedure was followed to obtain accurate transpiration values at the tree scale, as summarized in Appendix 1, other details can be found in Rana et al. (2023) and Ferrara et al. (2023).

Since E_p measurements were referred to the projected canopy area, transpiration by TDM at field scale was calculated as

$$E_{\text{TDM}} = A_p \overline{E_p}, \quad (4)$$

where E_{TDM} is expressed per unit of projected canopy area, i.e., kg m^{-2} or mm , with $\overline{E_p}$ the mean of the monitored trees and A_p the cover fraction, i.e., the area occupied by the mean vertical projection of each tree (Lu et al. 2003). A_p was determined every 2–5 days with the aid of images from the European Space Agency's Sentinel 2 satellite; with the application released by ESA, SNAP, the Coverage Fraction (FVC) was calculated (Sentinel 2 ToolBox; Level2 Products; Date Issued: 02.05.2016; Issue: V1.1. https://step.esa.int/docs/extra/ATBD_S2ToolBox_L2B_V1.1.pdf). Determinations on a daily time scale were calculated by integrating transpiration at the daytime (i.e., when $R_g > 10 \text{ W m}^{-2}$).

Transpirations at the field level in the two irrigation treatments are indicated by E_{SI} and E_{RDI} (mm).

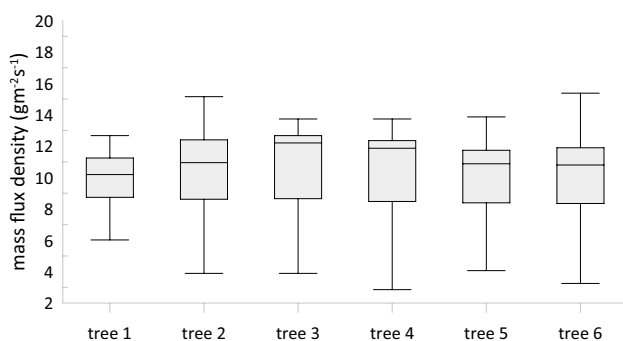


Fig. 1 Box plot of mean daily values of mass flux density for all monitored plants in the period March–June 2019

To estimate transpiration at seasonal and annual scales, a gap-filling strategy was developed by following Peters et al. (2010) and Rana et al. (2020). For each replicate tree, when 10-min J_i data were sporadically missing, J_i was calculated by linear interpolation; when more than 50% of daytime 10-min data were missing, the whole day was removed. Gaps in daily data were filled by developing a model for the relationship between J_i daily mean, daily mean VPD and daily cumulated R_g . The resulting functions for the two treatments were multivariate, quadratic in VPD and linear in R_g and were built using the procedure described by Rana et al. (2020).

Physiological variables and soil water content

Due to the hard pruning applied in March 2020, bearing shoot biomass was reduced, therefore, physiological and yield measurements were not carried out during this second season. Much better bearing shoot biomass and leaf surface of the olive orchard were achieved in the following 2021–2022 season.

During two vegetative growing seasons (2019–2020 and 2021–2022), to determine the difference in the water status of the plants, especially during the RDI period, simultaneous measurements of stem water potential (Ψ_s) and stomatal conductance (g_s) were carried out around midday (between 11:00 and 13:00 h solar time), every one/three weeks. The first plant for starting each cycle of measurements was chosen randomly each time, performing first the measurements on the east side of the plot, alternating SI and RDI treatments. These two variables were monitored from mid-June until mid-September, when the atmospheric demand in the region is elevated (Rana and Katerji 2000; Katerji et al. 2017).

Ψ_s was determined using a Scholander pressure chamber connected to a cylinder containing nitrogen. For each treatment, measurements were performed on 10 mature and fully expanded leaves (5 facing East and 5 facing West). The leaves were sealed with an aluminium bag for at least 1–2 h to prevent transpiration and allow them to reach equilibrium with water potential in the stem (McCutchan and Shackel 1992). Subsequently, they were cut near the base of the petiole and immediately measured.

Stomatal conductance was measured on the same days and time as Ψ_s determination. Two healthy, well-light-exposed leaf per tree (on the West and East side) selected at eye height were used to measure g_s for water vapour ($\text{mol}_{\text{H}_2\text{O}} \text{m}^{-2} \text{s}^{-1}$) using a portable open gas-exchange system fitted with a LED light source (LI-6400XT, LI-COR, Lincoln, NE, USA). During each measurement and on each side of the canopy, light intensity was maintained constant across the two treatments by setting the LED light source at the natural irradiance detected near the leaf. For each treatment, g_s

measurements were performed on the three plants where transpiration was measured by TDM and on two other trees that were similar in dimension, vigour and health state, chosen in correspondence with the soil moisture probes. The data were subjected to one-way ANOVA using SAS/STAT 9.2 software package (SAS/STAT 2010).

Soil water content in volume (θ , m^3m^{-3}) was measured by capacitive probes (5TM, Decagon Devices Inc., USA). For each treatment, three points were monitored: two points along the row (θ_r) and one between the rows (θ_{ir}). At each point, two capacitive probes were installed horizontally into the soil profile and transversely to the row, at -0.12 and -0.37 m from the soil surface, to intercept the dynamics of θ below the dripping lines. All sensors were connected to data-loggers (Tecno.el srl, Italy) and data were transferred to a web server via GPRS mode. Integrated soil–water content on a daily basis (θ_i) was determined for the soil profile (0.5 m) by integrating the values measured at each depth, since each probe was supposed to detect the water content in a 0.25 m soil layer (Campi et al. 2019), as:

$$\int_0^{0.5} \theta_i = \theta_{i(-0.12)} \cdot 0.25 + \theta_{i(-0.37)} \cdot 0.25. \quad (5)$$

The θ_i measurements from the three points were pooled to obtain a single average value for each treatment as (Searles et al. 2009; Autovino et al. 2018):

$$\theta = 0.7\bar{\theta}_r + 0.3\theta_{ir}, \quad (6)$$

where $\bar{\theta}_r$ is the mean of the two θ measured along the rows.

Soil water availability was described through the relative extractable water (REW, unitless) calculated using the average soil water content across positions around the tree and soil layers as

$$\text{REW} = \frac{\theta - \theta_{\min}}{\theta_{\max} - \theta_{\min}}, \quad (7)$$

where θ_{\min} is the minimum soil water content observed during the experiment and θ_{\max} is the maximum soil water content in the area (e.g., at field capacity).

Water stress and water use efficiency at canopy level

Water stress index (CWSI, unitless) at canopy level can be computed in function of the actual and potential transpirations (e.g., Jackson et al. 1981; Stanghellini and De Lorenzi 1994; Rana et al. 2020) as:

$$\text{CWSI} = 1 - \frac{E_{\text{TDM}}}{E_{\text{pot}}}, \quad (8)$$

where E_{TDM} is the transpiration measured by TDM as above described and E_{pot} is the potential transpiration calculated by a Penman–Monteith method approach (Appendix 2). CWSI ranges between 0 (no stress, with $E_{\text{TDM}} = E_{\text{pot}}$) and 1 (stress, with $E_{\text{TDM}} = 0$).

According to Fernández et al. (2020), SHD olive orchard water use efficiency and productivity at seasonal scale can be calculated as:

$$\text{WUE} = \frac{E_{\text{TDM}}}{P + I}, \quad (9a)$$

$$\text{WP} = \frac{\text{Yield}}{E_{\text{TDM}}}, \quad (9b)$$

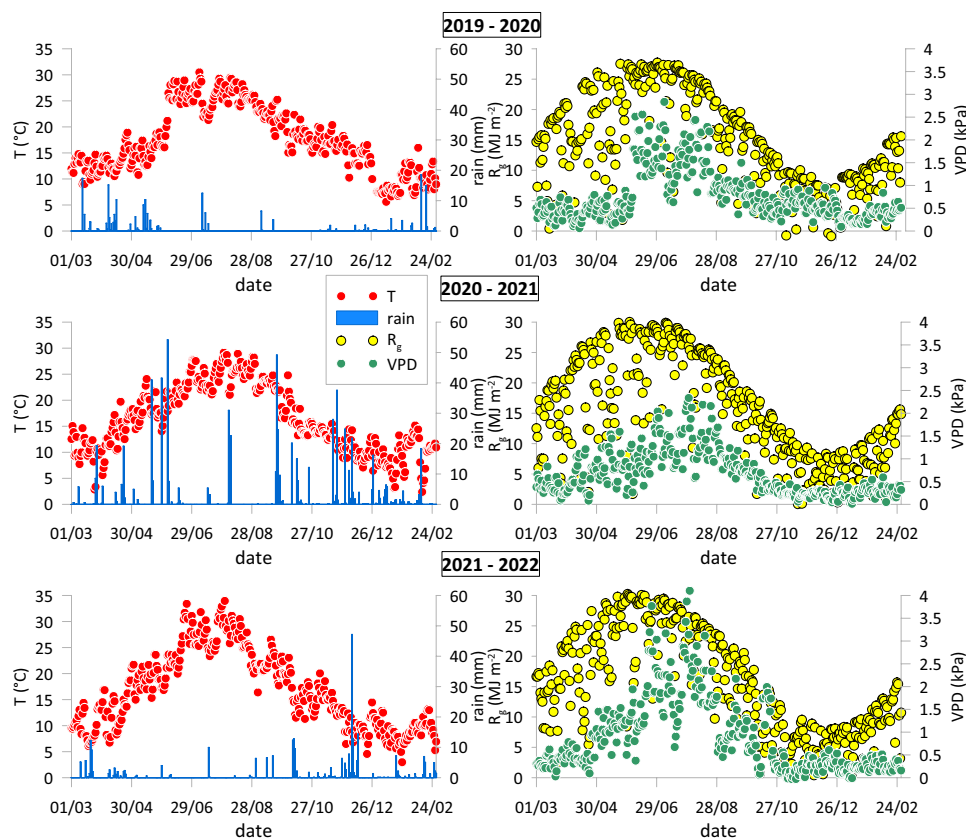
where E_{TDM} is total seasonal transpiration in $\text{kg}_{\text{H}_2\text{O}} \text{m}^{-2}$ (which is equivalent to mm of water) P and I are total precipitations and water supplied by irrigation in mm ($\text{kg}_{\text{H}_2\text{O}} \text{m}^{-2}$), yield is the marketable yield produced ($\text{kg} \text{m}^{-2}$). Yield values were determined in the first and third seasons (2019–2020 and in 2021–2022) as a mean of olives production measured on the same five trees used for physiological measurements. Harvesting times were yearly assessed by using ripening indices as reported by Camposeo et al. (2013).

Results and discussion

The weather and the actual transpiration

The seasonal time course of main agrometeorological parameters (T , VPD , R_g and P) during the three growth seasons is showed in Fig. 2, while Table 1 reports the seasonal values. The three seasons were characterized by very different weather, including extreme water scarcity conditions during 2019 and 2021 drought summers and the exceptionally rainy summer in 2020, characterized by few events of high rain intensity. 31 and 23 mm of rain fell in a few minutes on 5 and 7 August 2020, respectively; similarly, more than 100 mm of rain fell in three days between 21 and 23 September 2020. When rainfall was intense, waterlogging conditions were rarely achieved, due to the high hydraulic conductivity of the soil. The yearly mean air temperature was 18.1, 16.4 and 17.0 °C in 2019, 2020 and 2021, respectively, and was always warmer than in the past (15.6 °C). T was well above the mean in June 2019; an intense heat wave crossed the experimental field during summer 2021, between the end of July and the beginning of August when irrigation was withheld in the RDI plot. In summer 2022, mean T reached 34 °C, and peaks of 42 °C were observed during daytime. In these periods, VPD also reached high values, unusual for the region.

Fig. 2 Mean air temperature (T), sum rainfall (rain), sum global radiation (R_g) and mean (VPD) at daily scale in the three growth seasons



The *SPI* was equal to -1.61 , $+0.96$ and -1.45 for years 2019, 2020 and 2021, respectively, indicating that 2020 was extremely wet, while 2019 and 2021 were very dry, according to the cumulated precipitation. The greatly contrasted weather of the three seasons confirmed the strong variability following climate change in this Mediterranean area (Rana et al. 2016; Katerji et al. 2017).

Table 2 reports the water supply of each treatment in the three seasons: the RDI received 25, 22 and 33% less water with respect to SI, during the first, second and third season, respectively.

The actual transpiration trends in the three growth seasons at a daily scale are shown in Fig. 3, for SI and RDI treatments; the potential evaporation E_0 is also shown in Fig. 3. In the three seasons the orchard transpiration was mainly driven by the water atmosphere demand; in fact, E_{TDM} values increased from March until June, then slowly decreased until November, after that E_{TDM} remained quite constant and showed very low values until the end of January, when E_{TDM} values showed a tendency to increase again. E_{TDM} ranged between 0 and 2.73 mm for SI and between 0 and 1.95 mm for RDI, the same order as the values reported in other similar studies in the Mediterranean region (Tognetti et al. 2009; Camalleri et al. 2013; Chebbi et al. 2018). During the second growth season, the summer transpiration values were of the same order as the first season despite the

pruning. This can be explained by the weather conditions of 2020; in fact, the summer was particularly rainy, inducing a good water availability in the soil for crop transpiration (Fig. 4). Furthermore, during August, the combination of high wind speed and the thermodynamic status of atmosphere during the hottest hours of the day determine a high degree of coupling between vegetate surface and atmosphere (Rana et al. 2023; see also Supplementary Material II): the transpiration is less addressed by the canopy conductance and more by the available energy, which was particularly high under these conditions.

Following an ANOVA, in all growing seasons, E_{TDM} daily values for the two treatments were significantly not different ($p < 0.01$). Moving from SI to RDI, daily E_{TDM} was 0.68 and 0.73 mm, 0.68 and 0.72 mm, and 0.63 and 0.55 mm, in the first, second and third season, respectively, despite the RDI orchard received 124, 68 and 170 mm less irrigation water in the three seasons, respectively (Table 2). However, Fig. 2 clearly shows that olive trees under RDI treatment transpired less than SI during the period when irrigation was withheld in the first and in the third season, while the E_{TDM} values in SI and in RDI were quite similar in the second season due to the rainy summer (see Fig. 2) which effectively annulled the differentiation between the two irrigation regimes. Moreover, the reduction of E_{TDM} values due to the water withholding period appeared about 10–15 days after the stopping

Table 2 Yield, irrigation, transpiration (ETDM), water productivity (WP) and crop water use efficiency (WUE) of standard (SI) and regulated deficit (RDI) irrigation in the three growth seasons

Growth season	SI					RDI				
	Yield (kg m ⁻²)	Irrigation (kg m ⁻²)	ETDM (mm)	WP (g kg ⁻¹)	WUE	Yield (kg m ⁻²)	Irrigation (mm)	ETDM (mm)	WP (g kg ⁻¹)	WUE
2019–2020	0.67 ± 0.11	499	249	1.34	0.35	0.62 ± 0.12	375	267	1.64	0.45
2020–2021		306	249		0.25		238	262		0.28
2021–2022	0.41 ± .16	509	231	0.80	0.29	0.51 ± 0.14	339	202	1.50	0.32

of irrigation. This feature supports the results of Agüero Alcaras et al. (2016) and Corell et al. (2022), who found that transpiration in olive trees did not start to decline until much later than the water withholding.

Total seasonal transpirations were quite similar for both irrigation treatments in the three seasons (Table 2). The lowest total transpiration in the 2021–2022 growth season can be attributed to the extremely dry and warm weather conditions during spring and summer 2021 (see Fig. 2); indeed, in hedgerow olive orchards, E_{TDM} values show a diurnal relation with VPD, with a high logarithmic relationship between E_{TDM} and VPD (Zuñiga et al. 2014).

As reported in many other studies (see for example Tognetti et al. 2009; Katerji and Rana 2011), the measured E_{TDM} was strongly related to the weather variables driving crop transpiration (i.e., VPD and R_g ; Supplementary Material). E_{TDM} is significantly ($p < 0.01$) related to VPD by logarithmic functions in any growth season. While the linear relationships between E_{TDM} and R_g are significant ($p < 0.01$) in any season, indicating that any solar saturation value is advisable in this type of olive orchard.

Water use–soil and canopy scale

The REW trends at a daily scale in the three growth seasons are shown in Fig. 4, together with irrigations and precipitations, for both treatments. Gaps in values are due to the malfunctioning of soil moisture probes. In both treatments, REW increased immediately after water supply or rainfall and, conversely, decreased rapidly due to plant transpiration. In the RDI treatment, plants water recovery after the irrigation interruption period was quite fast, occurring around the same day of watering (Fernández 2014).

According to irrigation scheduling, before and after the irrigation withholding period, water supply results are the same in SI and in RDI. During these periods, SI and RDI trends are almost superimposable. Minor differences are due to the different total water availability in the two plots (0.105 and 0.122 m³ m⁻³ for SI and RDI, respectively) and to different minimum values of θ in the two soils (0.119 and 0.125 m³ m⁻³ for SI and RDI, respectively).

Several studies report a threshold of REW around 0.4 for indicating soil water deficit of woody species in arid and semiarid Mediterranean conditions (Bréda et al. 1995; Fernández et al. 1997; Grossiord et al. 2015). In the SI treatment, REW values ranged from 0.2 to 0.8 for most of the irrigation season, indicating soil water conditions far from the field capacity, except for short periods immediately after frequent irrigations and/or heavy precipitations. In the RDI treatment, REW values decreased when the irrigation supply was reduced. The minimum REW values in RDI treatment were 0.00, 0.17 and 0.20 in the first, second and third season, respectively. During the RDI period, REW values fell below

Fig. 3 Trends of actual transpiration (E_{TDM}) at daily scale, measured in the two treatments, standard irrigation (SI) and regulated deficit irrigation (RDI), during the three growth seasons, together with irrigation values. The potential Evaporation (E_0) is also shown. The RDI period (irrigation withholding period) is indicated by a light pink

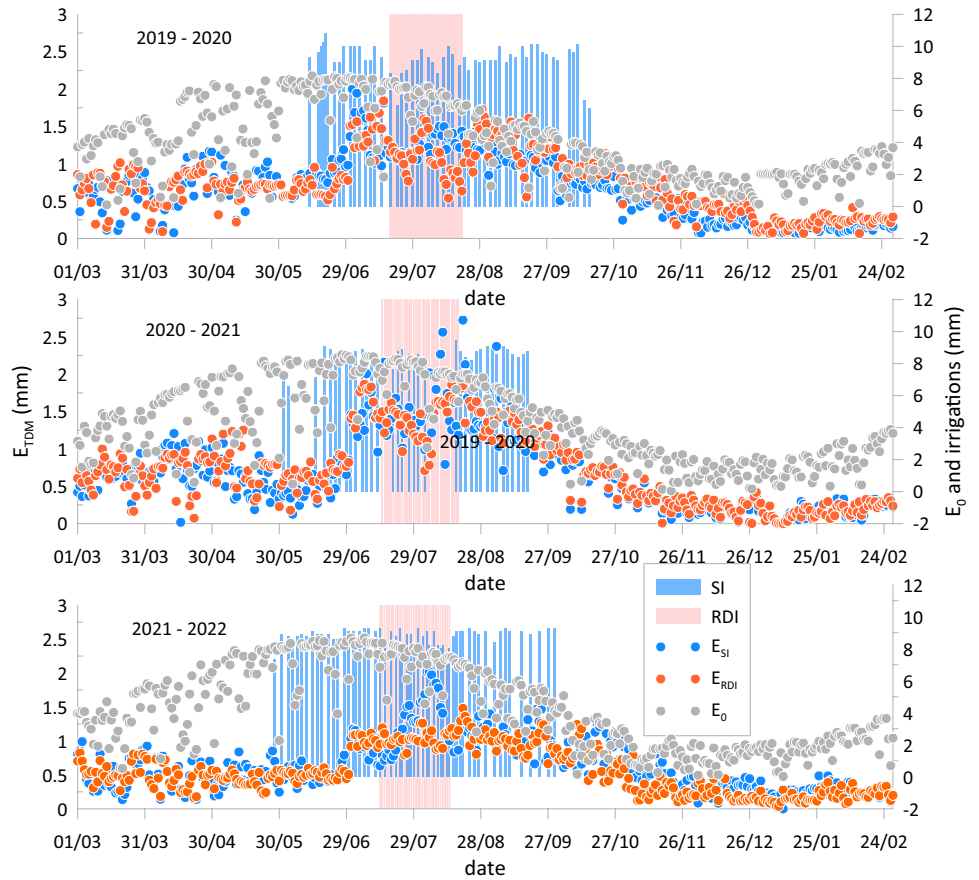
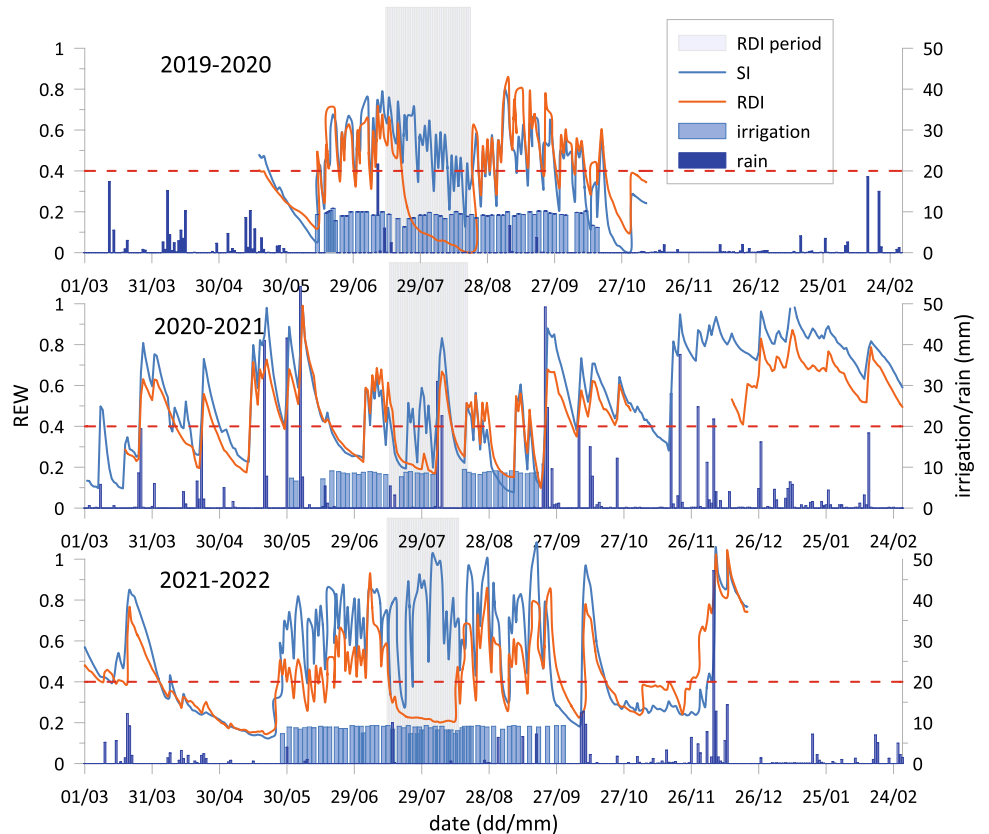


Fig. 4 The relative extractable water (REW, unitless) daily trend in the three growth seasons in both standard irrigation (SI) and regulated deficit irrigation (RDI) treatments; irrigation and precipitations are also reported. The horizontal dashed red line at $REW = 0.4$ indicates the threshold for water stress by literature (Bréda et al. 1995; Fernández et al. 1997; Grossiord et al. 2015). The RDI period (irrigation withholding period) is indicated by light grey



0.4 for 8 and 31 days in the first season, 19 and 26 days in the second season and 4 and 30 days in the third season in the SI and RDI treatments, respectively. In season 2020–2021, REW values lower than 0.4 were observed starting in spring: from 4 April 4 until 26 May, values below 0.4 were recorded for 52 and 53 days in the SI and RDI treatments, respectively. These results, and the effective water demand of the atmosphere (see Fig. 3), suggest that in the second season 2020–2021 the irrigation should have started a month earlier (in April instead of May), and the low E_{TDM} values during these months could be attributed to the decreased water availability in the soil.

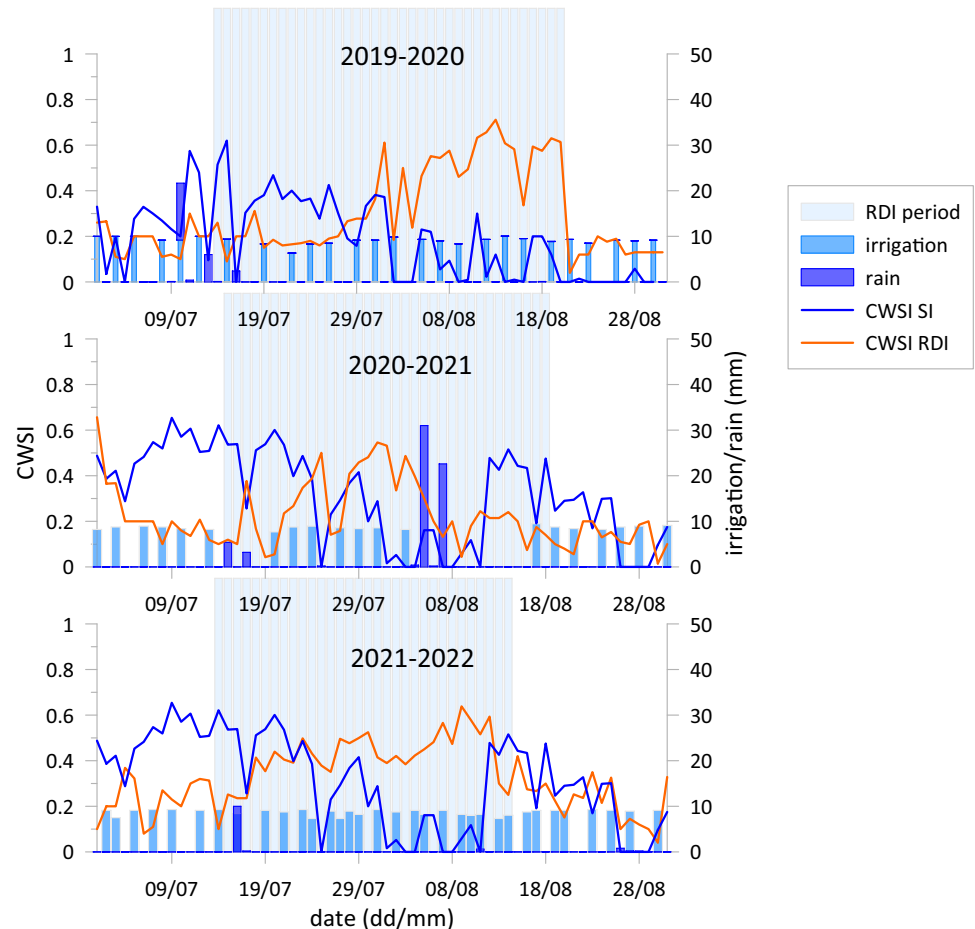
E_{TDM} was hardly increasing in spring (see Fig. 3) because the phenological phases in this period (woody buds breaking and shooting) involve intense water uptake by roots. On the contrary, the slight reduction in REW values in the fall did not seem to affect E_{TDM} because similar values were observed in 2020 when REW values were much higher than 0.4; in this case E_{TDM} reduction could be due to the physiological olive tree rest, starting from fruit ripening, induced by low temperatures (López-Bernal et al. 2020).

Due to the mathematical expression used to calculate CWSI (see Eq. (8)), steep oscillations in CWSI values were

observed when E_{TDM} and E_0 values were both close to zero, even though these oscillations did not have any physical significance. Therefore, for clarity, the daily CWSI is shown only for the dry months of July and August, during the RDI period in the three growing seasons (Fig. 5).

Focusing on the RDI period, during the first season, the mean CWSI value was quite higher for RDI (0.39) than SI (0.20). However, the CWSI values for RDI were generally far from 1. During the second season, the RDI crop was in a water condition closer to that of the SI crop (mean CWSI equal to 0.21 and 0.26 for SI and RDI, respectively). These results contrast with those reported by Egea et al. (2016) and Agam et al. (2013) who found clearly differentiated CWSI values in full irrigation and a similar RDI treatment in an SHD olive orchard in the Mediterranean region, although their CWSI was determined by infrared thermometry. Moreover, the mean CWSI values at the growth seasonal level were quite similar for the SI and RDI treatments (0.51 and 0.58, 0.54 and 0.63, 0.72 and 0.67 in the first, second and third season, respectively). These values can suggest that the water atmospheric demand and the coupling between this canopy and the atmosphere could play an important role. In fact, Rana et al. (2023) found that this hedgerow olive

Fig. 5 The crop water stress index (CWSI) trend during July and August in the three growth seasons in both standard irrigation (SI) and regulated deficit irrigation (RDI) treatments; irrigation and precipitations are also graphed. The RDI period (irrigation withholding period) is indicated by light grey



plantation is generally very well coupled to the atmosphere, regardless of soil water conditions. Furthermore, Tognetti et al. (2004) indicated that the large root system of olive trees might buffer reductions in relative extractable water, thus maintaining sufficient water supply with minor consequences on plant water relations.

Furthermore, the differences in CWSI values between treatments can suggest searching for a relationship with a specific plant water stress indicator as the stem water potential; the comparison between CWSI and Ψ_s , using all available data, (data not illustrated) shows a quadratic relationship ($R^2=0.44$), with an increasing of CWSI values at the decreasing of Ψ_s . This relationship is comparable with results by Egea et al. (2017), even if in our case the Ψ_s measured values range is limited, being between -1.0 and -2.2 MPa (see following). In Egea et al. (2017) the relationship between CWSI and Ψ_s is clearer than our data, maybe because the CWSI was determined by infrared thermometry, so with a variable also linked to the plant water status and measured at the same time. Therefore, a relation between CWSI and REW, both determined at a daily scale, can be profitably searched for here. In fact, if the attention is focused on the RDI treatment during the irrigation interruption period, a relationship between REW and CWSI can be detected (Fig. 6) during the period July–August. CWSI and REW are well related by statistically significant functions ($p < 0.01$) in the first and third seasons, while the correlation is not statistically significant in the second season when rainfalls affected the irrigation withholding period. Nevertheless, while in the first season CWSI values were high at a REW threshold value of 0.4 indicating crop stress, in the third season CWSI values were high only at REW threshold values below 0.5–0.6. In this case, it seems that the high evaporative demand of the atmosphere (very high VPD and T , see Fig. 2) prevails over the water availability of the soil in adapting the olive trees to serve water (Chirino et al. 2011), addressing the plants to decrease the transpiration by stomatal regulation (Fernández et al. 1997; Fernández 2014; Rana et al. 2023).

Water use–plant scale

Midday water potential and stomatal conductance from mid-June to mid-September are reported in Fig. 7.

In the first season, 2019–2020, Ψ_s for the SI treatment remained almost constant (-1.09 ± 0.12 MPa) throughout the period, while it progressively decreased in the RDI treatment during the irrigation interruption period, reaching the lowest value (-2.21 MPa) at the end of July. In the first three days of 2019–2020 season, as expected, no significant differences in g_s values were found between the treatments. On 31 July and 20 August, when the irrigation was interrupted in RDI, g_s was significantly higher in SI than

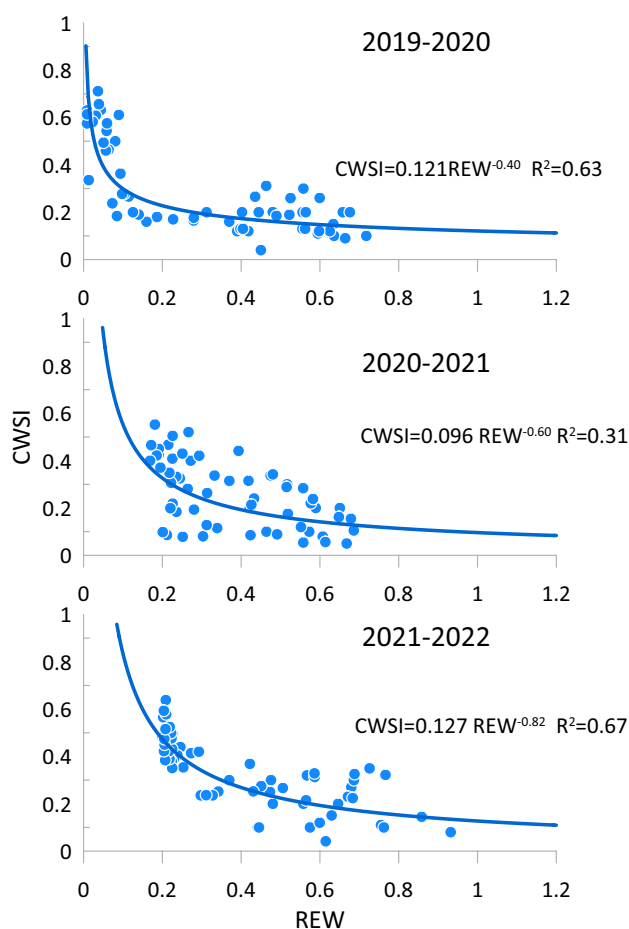
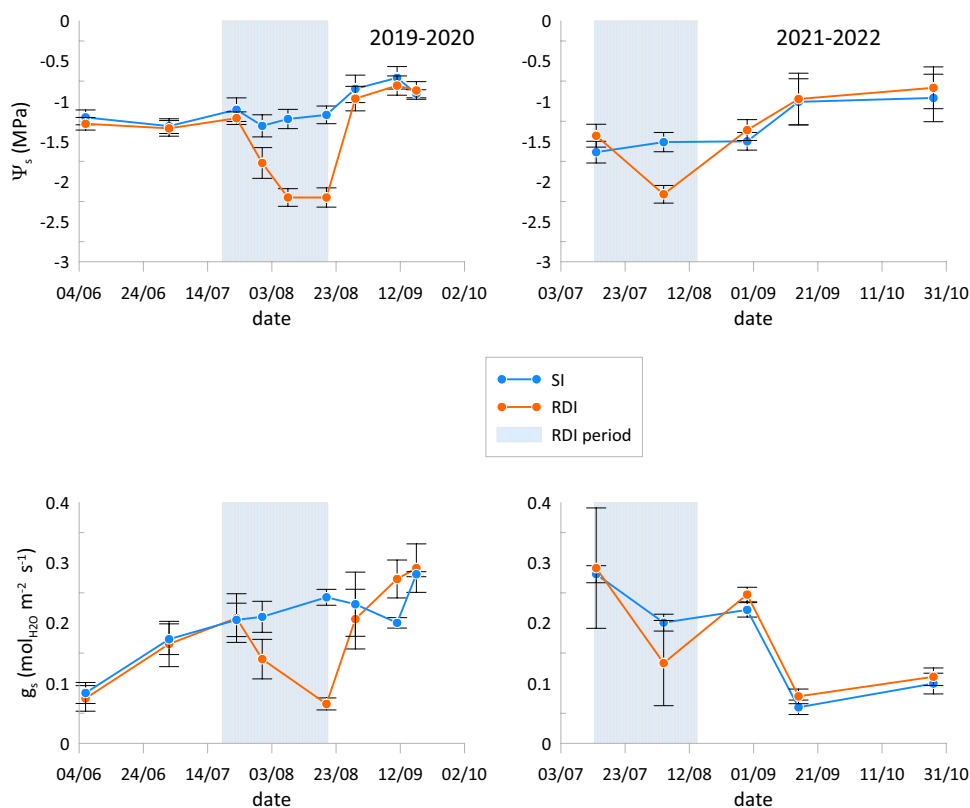


Fig. 6 Relationships between crop water stress index (CWSI) and relative extractable water (REW) in the period July–August for the regulated deficit irrigation (RDI) treatment in the three growth seasons

RDI ($p < 0.004$ and $p < 0.0001$ on 31 July and 20 August, respectively). The RDI treatment showed an increase in g_s when irrigation was resumed, demonstrating a full recovery and even surpassing the SI treatment on 11 September ($p < 0.004$), in accord with Fernández et al. (1997). In the first growing season, g_s for SI treatment roughly increased from June to September, reaching a maximum value of $0.28 \text{ mol}_{\text{H}_2\text{O}} \text{ m}^{-2} \text{ s}^{-1}$; g_s for RDI treatment decreased during the irrigation interruption period, reaching a minimum value of $0.07 \text{ mol}_{\text{H}_2\text{O}} \text{ m}^{-2} \text{ s}^{-1}$ in correspondence of the lowest Ψ_s values in mid-August.

In the third season, Ψ_s for the SI gradually and slowly increased from mid-July, being in mean equal to -1.32 ± 0.19 MPa; Ψ_s for RDI treatment decreased during the irrigation interruption period until the minimum value of -2.16 MPa at the beginning of August. In the third season, Ψ_s mean value of SI treatment was quite close to the mean value of RDI treatment (-1.35 ± 0.19 MPa) indicating that the two plots were in closer water conditions than in the first season. In the third season, in general, the trend of g_s

Fig. 7 Stem water potential (Ψ_s) and stomatal conductance (g_s) measured at midday in the first (2019–2020) and third season (2021–2022) in standard irrigation (SI) and regulated deficit irrigation (RDI) treatments. The RDI period (irrigation withholding period) is indicated by light grey



for the SI and RDI treatments was non-statistically different, indicating similar crop water status, as also reported by the behaviour of water potential. During the RDI period, stomatal conductance in SI was significantly higher than RDI (4 August, $p < 0.0001$). In the summer of 2021–2022 season, the lowest g_s values in SI and RDI were reached at the beginning of September (0.06 and $0.07 \text{ mol}_{\text{H}_2\text{O}} \text{m}^{-2} \text{s}^{-1}$, respectively) when the REW dropped dramatically, T and VPD were still high, affecting the stomata regulation as indicated by Zhang et al. (2019). These results suggest that stomatal conductance measured at the leaf level could be used as a water stress indicator (Hernandez-Santana et al. 2016) in *Arbosana* olive cultivar. Both eco-physiological parameters indicate that the olive tree has a good ability to recover from water stress when soil moisture is replenished. Indeed, depending on the severity of the water stress, until -2.5 MPa of Ψ_s olive eco-physiological recovery occurs within 2–3 days; between -2.4 and -4.0 MPa recovery occurs within 20–30 days; it never occurs over -4.0 MPa (see Angelopoulos et al. 1996; Fernández et al. 1997; Alegre et al. 1999; Moriana et al. 2002; Sofo et al. 2008; Iniesta et al. 2009).

The relationship between stem water potential and stomatal conductance is shown in Fig. 8, which includes all values simultaneously measured. This relationship indicates that the RDI orchard was always in low/mild-moderate water stress and the SI orchard is in low water stress conditions

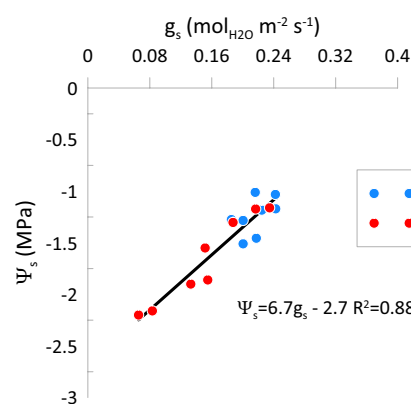


Fig. 8 Relationship between stem water potential (Ψ_s) and stomatal conductance (g_s) measured at midday in standard irrigation (SI) and regulated deficit irrigation (RDI) treatments; all available measurements are plotted

(Ahumada-Orellana et al. 2019). Under these conditions, this SHD olive orchard adjust its water consumption as soon as the thermodynamic conditions of the atmosphere become such as to require a costly increase in transpiration, even at water contents far from the wilting point ($0.183 \text{ m}^3 \text{m}^{-3}$). In this way, the olive trees avoid reaching high water potential values that produce a loss of hydraulic conductivity (Tognetti et al. 2009), thus preventing irreversible damage (Vilagrosa et al. 2003; Hernandez-Santana et al. 2016).

Water use efficiency and water productivity

The WUE and WP values for the three experimental seasons are reported in Table 2: the RDI treatment presents higher WUE and WP values than SI treatment. In 2020–2021 season, the olive orchard did not yield due to necessary hard rejuvenation pruning.

The RDI WUE, which used an average of 83% of the SI water, was 16% higher than the WUE for the SI treatment. The results are consistent with the finding of Fernández et al. (2013), who observed increases in WUE of 20% and 32% for 60% and 30% RDI, respectively, for *cv. Arbequina* in Spain. Padilla-Díaz et al. (2018) also found an increase of 32% in WUE for a 45% RDI treatment with respect to the full irrigation treatment in the same site and olive cultivar. Finally, it is difficult to compare the WP values in this study to those of other investigations in similar hedgerow olive orchards because whole-season measurements of actual transpiration, as were conducted in this study, are rare (Chebbi et al. 2018).

Conclusions

In this study, the cumulated value of water transpired at the growth seasonal scale was compared for an SHD olive orchard under standard irrigation versus regulated deficit irrigation. The trial was carried out for three years (1096 days) in a Mediterranean site with one of the most widely cultivated olive genotype in SHD olive orchards (*cv. Arbosana*). The total transpiration values at the season–year time scales were obtained by continuous measurements applying the sap flow thermal dissipation method in a rigorous manner (Ferrara et al. 2023); in particular, since the used probe were 20 mm length, a specific Gaussian function was applied to take into account the gradient effects in the sapwood area.

RDI regime applied to the SHD olive orchard reduced water requirements, did not affect olive yields and improved water use efficiencies. The 38% reduction in irrigation water applied to the RDI, compared to SI, had a weak or null effect on the physiological response of olive trees at a seasonal time scale. Therefore, RDI is a water-saving technique that should further increase the environmental sustainability of SHD olive orchards with well-adapted cultivars. Finally, these are the first eco-physiological data that took into account the rejuvenation pruning of an adult SHD olive orchard, supplying more insights into the behaviour of the well-adapted cultivars.

The relative extractable water value of 0.4, usually indicated as a stress threshold value, for this olive SHD orchard was not an absolute value, but depended on the atmospheric conditions, i.e. its water demand.

At the plant scale, during the RDI period, the SHD olive trees adjusted their stomatal conductance as soon as stem water potential was threatened, avoiding high water potential values that could lead to irreversible damage through a loss of hydraulic conductivity. Stomatal conductance at the leaf level could be used as a water stress indicator due to its strong relationship with stem water potential.

The results of this study indicated that the olive tree has good water recovery ability in SHD orchards under RDI, with stem water potential never exceeding -2.5 MPa and eco-physiological recovery occurring within a few days after water supply is restored.

Appendix 1: Specific calibration of TDM and the correction factors

The mass flux density (J_i , $\text{gm}^{-2} \text{s}^{-1}$) was determined by the relation (Granier 1985; Lu et al. 2003):

$$J_i = aK^b, \quad (10)$$

with a and b determined by specific local calibration. According to Alarcón et al. (2005), McCulloh et al. (2007) and Zhou et al. (2017), the calibration to find the specific coefficients a and b in the Eq. (10) was carried out on three 5-year-old trees of the investigated variety (*Arbosana*) cultivated in pots placed in plastic cylindrical pots. The calibration curve is obtained plotting the J_{s0} of Eq. (4) vs the K values, obtaining for a and b the values (Supplementary Material IV):

$$J_i = 140K^{1.118}. \quad (11)$$

To have suitable sap flow measurements for correct plant water consumption, the mass flux density measured in each sampled tree was corrected for (i) the effect of wounds; (ii) the effect of azimuthal variations; (iii) the effect of gradient (inside the sapwood from the youngest to oldest channels). For each of the above-mentioned three corrections, the coefficients were calculated in the period June–August 2022, after the experiment (Ferrara et al. 2023).

A coefficient C_w was determined to correct the mass flux density for the wound effects (Wiedemann et al. 2016) as:

$$J_i = 140(C_w K)^{1.118}. \quad (12)$$

For this aim, a couple of TDM probes (20 mm), one heated and one unheated, were installed in parallel to the already measuring probes (installed in the first part of January 2021) in two trees, at the same height and 20 mm from the already installed ones, in the period 23 June–23 August 2022. Hence, since the wound effect is due to the

probe insertion in the trunk and then, affects the measured ΔT , correction is limited to the K parameter.

The azimuthal variations of mass flux density were analysed in two sampled trees by calculating a correction coefficient C_a , as reported in Shinohara et al. (2013); therefore, the mass flux density is now:

$$J_i = C_a a (C_w K)^b \quad (13)$$

The azimuthal variations of sap flux density were analysed in two sampled trees, by adding two couples of TDM probes (20 mm) at 120° and 240° , in the period 23 June–23 August 2022. For considering this azimuth effect we followed Shinohara et al. (2013), to extrapolate sap flux density in the north direction, using the north sensor as a reference to the three integrated directions (averaged over the three directions). Hence, the correction coefficient is calculated as the ratio of the mean sap flux density in the three directions to the sap flux density in the north direction.

Finally, to account for a radial gradient in sap flux density, the sapwood depth of each sampled tree was divided in a set of 20 mm increments and a Gaussian function was applied to estimate the sap flux density in each increment as suggested by Pataki et al. (2011) for angiosperms and verified in the field:

$$J_{si} = 1.033 J_i \exp \left[-0.5 \left(\frac{x - 0.09963}{0.4263} \right)^2 \right], \quad (14)$$

where J_{si} is the sap flux density in each increment i , x is the normalized depth of each sapwood increment ($0 \leq x < 1$) and J_i is calculated using Eq. (6).

Here, to test the used function (Eq. 14) over the active sapwood (Rana et al. 2020), two new set of TDM probe were installed in parallel to the already measuring probes in two sampled trees, at the same height and 20 mm from the other ones, in the period 23 June–23 August 2022. In this case, beyond the 20 mm probes, commercial sap flow probes of 10 mm length (SFS2 Type M, UP, Steinfurt, Germany) were installed. From the sap flow density measured from the couple of probes the J_i values in the layer 10–20 mm of the sapwood depth was derived according to Iida and Tanaka (2010) as follows:

$$J_{s10-20} = \frac{J_{s0-20} - \alpha J_{s0-10}}{\beta}, \quad (15)$$

where α and β are the proportions of the sapwood area from depths of 0–10 mm to that of 0–20 mm, and from depths of 10–20 mm to that of 0–20 mm, respectively.

Finally, the whole tree transpiration of each sampled tree (E_p , g s^{-1}) was determined as:

$$E_p = \sum_{i=0}^m J_{si} \text{SWA}_i, \quad (16)$$

where m is the number of 20-mm increments in sapwood depth, J_{si} is the sap flux density determined by Eq. (14) and SWA_i is the sapwood area at each depth increase i .

Appendix 2: the potential transpiration

Potential transpiration (E_{p0}) for this olive orchard is calculated by the Penman–Monteith model under this form:

$$E_{p0} = \frac{1}{\lambda} \frac{\epsilon r_a A + \rho c_p \text{VPD}/\gamma}{(1 + \epsilon)r_a + r_{c, \min}}, \quad (17)$$

with λ (MJ kg^{-1}) being the latent heat of water vaporization, r_a the aerodynamic resistance (s m^{-1}), $r_{c, \min}$ is the minimum canopy resistance (s m^{-1}), fixed to 65 s m^{-1} (Villalobos et al. 2000), ρc_p the volumetric heat capacity of air ($\text{J m}^{-3} \text{K}^{-1}$), A is the energy available to the canopy (W m^{-2}), VPD is the vapor pressure deficit of the air (kPa), γ is the psychrometric constant (kPa K^{-1}) and $\epsilon = \Delta/\gamma$ is the rate of change of latent heat content with sensible heat content of saturated air (kPa K^{-1}). Since the use of Eq. (17) implies already a simplified representation of the behaviour of the real canopy, i.e. the adoption of a “big leaf” model (i.e., Monteith 1965; Sellers et al. 1996), here we accurately determined all terms to reduce the inaccuracies in the calculation of E_{p0} .

Since E_{p0} should be referred to the canopy site, and the weather variables were measured in a separate meteorological station, Rana and Katerji (2008) was followed; details on the approach can also be found in Rana et al. (2023). After a local calibration of 12 months (January–December 2021), G was considered as a constant at the daily scale and equal to $0.09 R_n$.

Supplementary Information The online version contains supplementary material available at <https://doi.org/10.1007/s00271-023-00892-5>.

Author contributions Conceptualization: GR; Methodology: GR, RMF; Investigation: GR, MRB, PC, LG, SR, GD, NM, AFM, TM, MP; Formal analysis: GR, RMF, CS; Writing—original draft preparation: GR, RMF; Writing—review and editing: GR, RMF, SC; Funding acquisition: MM.

Funding This study was funded by and carried out within the MOLTI project (Decree n. 13938, 661 April the 24th 2018) funded by the Italian Ministry of Agriculture (MiPAAF).

Data availability Data are available under request to the authors. Pictures and descriptions of used equipment are available under request.

Code availability Not applicable.

Declarations

Conflict of interest The authors, Rossana Monica Ferrara, Maria Roberta Bruno, Pasquale Campi, Salvatore Camposeo, Gabriele De Carolis, Liliana Gaeta, Nicola Martinelli, Marcello Mastrorilli, Anna Francesca Modugno, Teresa Mongelli, Mariagrazia Piarulli, Sergio Ruggieri, Gianfranco Rana declare no conflict of interest.

Ethics approval Not applicable.

References

- Agam N, Cohen Y, Berni JA, Alchanatis V, Kool D, Kool D, Dag A, Yermiyahu U, Ben-Gal A (2013) An insight to the performance of crop water stress index for olive trees. *Agric Water Manag* 118:79–86. <https://doi.org/10.1016/J.AGWAT.2012.12.004>
- Aganchich A, Tahi H, Wahbi S, Elmodaffar C, Serraj R (2007) Growth, water relations and antioxidant defence mechanisms of olive (*Olea europaea* L.) subjected to Partial Root Drying (PRD) and Regulated Deficit Irrigation (RDI). *Plant Biosyst* 141(2):252–264. <https://doi.org/10.1080/1126350070141893>
- Agüero Alcaras LM, Rousseaux MC, Searles PS (2016) Responses of several soil and plant indicators to post-harvest regulated deficit irrigation in olive trees and their potential for irrigation scheduling. *Agric Water Manag* 171:10–20. <https://doi.org/10.1016/J.AGWAT.2016.03.006>
- Aguilera F, Ruiz L, Fornaciari M, Romano B, Galán C, Oteros J, Ben Dhiab A, Msallem M, Orlandi F (2014) Heat accumulation period in the Mediterranean region: phenological response of the olive in different climate areas (Spain, Italy and Tunisia). *Int J Biometeorol* 58:867–876. <https://doi.org/10.1007/s00484-013-0666-7>
- Ahumada-Orellana LK, Ortega-Farías S, Poblete-Echeverría C, Searles PS (2019) Estimation of stomatal conductance and stem water potential threshold values for water stress in olive trees (cv. Arbequina). *Irrig Sci* 37:461–467. <https://doi.org/10.1007/s00271-019-00623-9>
- Ahumada-Orellana L, Ortega-Farías S, Searles PS, Zúñiga M (2023) Leaf gas exchange, water status, and oil yield responses to rewatering after irrigation cut-off periods in a superintensive drip-irrigated olive (cv. Arbequina) orchard. *Irrig Sci* 41(4):557–570. <https://doi.org/10.1007/s00271-022-00817-8>
- Alarcón JJ, Ortuño MF, Nicolás E, Torres R, Torrecillas A (2005) Compensation heat-pulse measurements of sap flow for estimating transpiration in young lemon trees. *Biol Plant* 49(4):527–532. <https://doi.org/10.1007/s10535-005-0046-1>
- Albarracín V, Hall AJ, Searles PS, Rousseaux MC (2018) Impact of simulated mechanical hedge pruning and wood age on new shoot demography and return flowering in olive trees. *Trees* 32(6):1767–1777. <https://doi.org/10.1007/s00468-018-1749-1>
- Alegre S, Girona J, Marsal J, Arbonés A, Mata M, Montagut D, Teixidó F, Motilva MJ, Romero MP (1999) Regulated deficit irrigation in olive trees. *Acta Hortic* 474:373–376. <https://doi.org/10.17660/ActaHortic.2002.586.49>
- Allen RG, Pereira LS, Raes D, Smith M (1998) Crop evapotranspiration. Guidelines for computing crop water requirements. FAO irrig drain paper No. 56, Rome, pp 300
- Allen RG, Pereira LS (2009) Estimating crop coefficients from fraction of ground cover and height. *Irrig Sci* 28:17–34. <https://doi.org/10.1007/s00271-009-0182-z>
- Angelopoulos K, Dichio B, Xiloyannis C (1996) Inhibition of photosynthesis in olive trees (*Olea europaea* L.) during water stress and rewatering. *J Exp Bot* 301:1093–1100. <https://doi.org/10.1093/jxb/47.8.1093>
- Autovino D, Rallo G, Provenzano G (2018) Predicting soil and plant water status dynamic in olive orchards under different irrigation systems with Hydrus-2D: model performance and scenario analysis. *Agric Water Manag* 203:225–235. <https://doi.org/10.1016/j.agwat.2018.03.015>
- Bouman BAM (2007) A conceptual framework for the improvement of crop water productivity at different spatial scales. *J Agric Food Syst Community Dev* 93:43–60. <https://doi.org/10.1016/j.agsy.2006.04.004>
- Bréda N, Granier A, Barataud F, Moyné C (1995) Soil water dynamics in an oak stand. *Plant Soil* 172:17–27. <https://doi.org/10.1007/BF00020856>
- Burgess SSO, Adams MA, Turner NC, Beverly CR, Ong CK, Khan AAH, Bleby TM (2001) An improved heat pulse method to measure low and reverse rates of sap flow in woody plants. *Tree Physiol* 21:589–598. <https://doi.org/10.1093/TREEPHYS/21.9.589>
- Cajias E, Antunez A, Román LF (2016) Response to moderate water stress imposed after pit hardening in mature table olive orchard cv. Azapa. *Agric Water Manag* 173:76–83. <https://doi.org/10.1016/j.agwat.2016.04.029>
- Cammalleri C, Rallo G, Agnese C, Ciruolo G, Minacapilli M, Provenzano G (2013) Combined use of eddy covariance and sap flow techniques for partition of ET fluxes and water stress assessment in an irrigated olive orchard. *Agric Water Manag* 120:89–97. <https://doi.org/10.1016/j.agwat.2012.10.003>
- Campi P, Mastrorilli M, Stellacci AM, Modugno F, Palumbo AD (2019) Increasing the effective use of water in green asparagus through deficit irrigation strategies. *Agric Water Manag* 217:119–130. <https://doi.org/10.1016/J.AGWAT.2019.02.039>
- Camposeo S, Godini A (2010) Preliminary observations about the performance of 13 varieties according to the super high density olive culture training system in Apulia (southern Italy). *Adv Hortic Sci* 24(1):16–20. <https://doi.org/10.1400/132338>
- Camposeo S, Vivaldi GA, Gattullo CE (2013) Ripening indices and harvesting times of different olive cultivars for continuous harvest. *Sci Hortic* 151:1–10. <https://doi.org/10.1016/j.scienta.2012.12.019>
- Camposeo S, Vivaldi GA, Russo G, Melucci FM (2022) Intensification in olive growing reduces global warming potential under both integrated and organic farming. *Sustainability* 14:6389. <https://doi.org/10.3390/su14116389>
- Chebbi W, Boulet G, Le Dantec V, Lili Chabaane Z, Fanise P, Mougnot B, Ayari H (2018) Analysis of evapotranspiration components of a rainfed olive orchard during three contrasting years in a semi-arid climate. *Agric Meteorol* 256–257:159–178. <https://doi.org/10.1016/J.AGRFORMET.2018.02.020>
- Chirino E, Bellot J, Sánchez JR (2011) Daily sap flow rate as an indicator of drought avoidance mechanisms in five Mediterranean perennial species in semi-arid southwestern Spain. *Trees* 25:593–606. <https://doi.org/10.1007/s00468-010-0536-4>
- Conceição N, Tezza L, Häusler M, Lourenço S, Pacheco CA, Ferreira MI (2017) Three years of monitoring evapotranspiration components and crop and stress coefficients in a deficit irrigated intensive olive orchard. *Agric Water Manag* 191:138–152. <https://doi.org/10.1186/s13601-019-0279-2>
- Corell M, Pérez-López D, Andreu L, Recena R, Centeno A, Galindo A, Moriana A, Martín-Palomo MJ (2022) Yield response of a mature hedgerow oil olive orchard to different levels of water stress during pit hardening. *Agric Water Manag* 261:107374. <https://doi.org/10.1016/j.agwat.2021.107374>
- Egea G, Diaz-Espejo A, Fernández JE (2016) Soil moisture dynamics in a hedgerow olive orchard under well-watered and deficit irrigation regimes: assessment, prediction and scenario analysis. *Agric Water Manag* 164:197–211. <https://doi.org/10.1016/j.agwat.2015.10.034>

- Egea G, Padilla-Díaz CM, Martínez-Guanter J, Fernández JE, Pérez-Ruiz M (2017) Assessing a crop water stress index derived from aerial thermal imaging and infrared thermometry in super-high density olive orchards. *Agric Water Manag* 187:210–221
- Espadafor M, Lorite IJ, Gavilán P, Berengena J (2011) An analysis of the tendency of reference evapotranspiration estimates and other climate variables during the last 45 years in Southern Spain. *Agric Water Manage* 98(6):1045–1061. <https://doi.org/10.1016/J.AGWAT.2011.01.015>
- Fernández J-E (2014) Understanding olive adaptation to abiotic stresses as a tool to increase crop performance. *Environ Exp Bot* 103:158–179. <https://doi.org/10.1016/J.ENVEXPBOT.2013.12.003>
- Fernández J-E, Moreno F, Girón IF, Blázquez OM (1997) Stomatal control of water use in olive tree leaves. *Plant Soil* 190:179–192. <https://doi.org/10.1023/A:1004293026973>
- Fernández JE, Perez-Martin A, Torres-Ruiz JM, Cuevas MV, Rodriguez-Dominguez CM, Elsayed-Farag S, Morales-Sillero A, García JM, Hernandez-Santana V, Diaz-Espejo A (2013) A regulated deficit irrigation strategy for hedgerow olive orchards with high plant density. *Plant Soil* 372:279–295. <https://doi.org/10.1007/s11104-013-1704-2>
- Fernández J-E, Alcon F, Diaz-Espejo A, Hernandez-Santana V, Cuevas MV (2020) Water use indicators and economic analysis for on-farm irrigation decision: a case study of a super high density olive tree orchard. *Agric Water Manag* 237:106074. <https://doi.org/10.1016/j.agwat.2020.106074>
- Ferrara RM, Campi P, De Carolis G, Gaeta L, Piarulli M, Ruggieri S, Rana G (2023) Transpiration by sap flow Thermal Dissipation Method: applicability to a hedgerow olive orchard. *Ital J Agrometeorol* 1:37–46. <https://doi.org/10.36253/ijam-1919>
- Fraga H, Moriondo M, Leolini L, Santos JA (2021) Mediterranean olive orchards under climate change: a review of future impacts and adaptation strategies. *Agronomy*. <https://doi.org/10.3390/agronomy11010056>
- Fuchs S, Leuschner C, Link R, Coners H, Schuldt B (2017) Calibration and comparison of thermal dissipation, heat ratio and heat field deformation sap flow probes for diffuse-porous trees. *Agric Forest Meteorol* 244–245:151–161. <https://doi.org/10.1016/j.agrformet.2017.04.003>
- García JM, Morales-Sillero A, Pérez-Rubio AG, Diaz-Espejo A, Monteroc A, Fernández J-E (2017) Virgin olive oil quality of hedgerow ‘Arbequina’ olive trees under deficit irrigation. *J Sci Food Agric* 97:1018–1026. <https://doi.org/10.1002/jsfa.7828>
- Giorgi F (2006) Climate change hot-spots. *Geophys Res Lett* 33:8707. <https://doi.org/10.1029/2006GL025734>
- Godini A, Vivaldi GA, Camposeo S (2011) Olive cultivars field-tested in super-high-density system in southern Italy. *Calif Agric* 65(1):39–40. <https://doi.org/10.3733/ca.v065n01p39>
- Goldhamer DA (1999) Regulated deficit irrigation for California canning olives. *Acta Hort* 474:369–372. <https://doi.org/10.17660/actahortic.1999.474.76>
- Granier A (1985) Une nouvelle méthode pour la mesure du flux de sève brute dans le tronc des arbres (A new method to measure sap flow in tree stems). *Ann Sci for (EDP Sciences)* 42(2):193–200
- Granier A (1987) Evaluation of transpiration in a Douglas-fir stand by means of sap flow measurements. *Tree Physiol* 3:309–320. <https://doi.org/10.1093/treephys/3.4.309>
- Grossiord C, Forner A, Gessler A, Granier A, Pollastrini M, Valladares F, Bonal D (2015) Influence of species interactions on transpiration of Mediterranean tree species during a summer drought. *Eur J Forest Res* 134:365–376. <https://doi.org/10.1007/s10342-014-0857-8>
- Hernández ML, Velázquez-Palmero D, Sicardo MD, Fernández JE, Diaz-Espejo A, Martínez-Rivas JM (2018) Effect of a regulated deficit irrigation strategy in a hedgerow ‘Arbequina’ olive orchard on the mesocarp fatty acid composition and desaturase gene expression with respect to olive oil quality. *Agric Water Manage* 204:100–106. <https://doi.org/10.1016/j.agwat.2018.04.002>
- Hernandez-Santana V, Fernández JE, Rodriguez-Dominguez CM, Romero R, Diaz-Espejo A (2016) The dynamics of radial sap flux density reflects changes in stomatal conductance in response to soil and air water deficit. *Agric for Meteorol* 218–219:92–101. <https://doi.org/10.1016/J.AGRFORMET.2015.11.013>
- Iida S, Tanaka T (2010) Effect of the span length of Granier-type thermal dissipation probes on sap flux density measurements. *Ann for Sci* 67:408
- Iniesta F, Testi L, Orgaz F, Villalobos FJ (2009) The effects of regulated and continuous deficit irrigation on the water use, growth and yield of olive trees. *Eur J Agron* 30:258–265. <https://doi.org/10.1016/J.EJA.2008.12.004>
- Jackson RD, Idso SB, Reginato RL, Pinter PJ Jr (1981) Canopy temperature as a crop water stress indicator. *Water Resour Res* 17:1133–1141. <https://doi.org/10.1029/WR0171004P01133>
- Kang Y, Khan S, Ma X (2009) Climate change impacts on crop yield, crop water productivity and food security—a review. *Prog Nat Sci* 19:1665–1674
- Katerji N, Rana G (2011) Crop reference evapotranspiration: a discussion of the concept, analysis of the process and validation. *Water Resour Manag* 25:1581–1600. <https://doi.org/10.1007/S11269-010-9762-1>
- Katerji N, Mastrorilli M, Rana G (2008) Water use efficiency of crops cultivated in Mediterranean region: review and analysis. *Eur J Agron* 28(4):493–507. <https://doi.org/10.1016/J.EJA.2007.12.003>
- Katerji N, Rana G, Ferrara RM (2017) Actual evapotranspiration for a reference crop within measured and future changing climate periods in the Mediterranean region. *Theor Appl Climatol* 129(3–4):923–938. <https://doi.org/10.1007/s00704-016-1826-6>
- Kokkotos E, Zotos A, Tsirogiannis G, Patakas A (2021) Prediction of olive tree water requirements under limited soil water availability, based on sap flow estimations. *Agronomy* 11:1318. <https://doi.org/10.3390/agronomy11071318>
- Lee X, Massman W, Law B (eds) (2004) Handbook of micrometeorology: a guide for surface flux measurement and analysis, vol 29. Springer, Berlin
- López-Bernal Á, García-Tejera O, Testi L, Orgaz F, Villalobos FJ (2020) Studying and modelling winter dormancy in olive trees. *Agric for Meteorol* 280:107776. <https://doi.org/10.1016/j.agrformet.2019.107776>
- Lu P, Yunusa IAM, Walker RR, Müller WJ (2003) Regulation of canopy conductance and transpiration and their modelling in irrigated grapevines. *Funct Plant Biol* 30:689–698. <https://doi.org/10.1071/FP02181>
- Masmoudi CC, Masmoudi M, Abid-Karray J, Ben Mechlia N (2011) Sap flow measurements in young olive trees (*Olea europaea* L.) cv. Chétoui under Tunisian conditions. *Sci Hort* 129:520–527. <https://doi.org/10.1016/J.SCIHORT.2011.05.030>
- McCulloh KA, Winter K, Meinzer FC, Garcia M, Aaranda J, Lachenbruch B (2007) A comparison of daily water use estimates derived from constant-heat sap-flow probe values and gravimetric measurements in pot-grown saplings. *Tree Physiol* 27:1355–1360. <https://doi.org/10.1093/treephys/27.9.1355>
- McCutchan H, Shackel KA (1992) Stem-water potential as a sensitive indicator of water stress in prune trees (*Prunus domestica* L. cv. French). *J Am Soc Hort Sci* 117(4):607–611
- Monteith JL (1965) Evaporation and environment. In: Symposia of the society for experimental biology, vol 19. Cambridge University Press (CUP), Cambridge, pp 205–234
- Moriana A, Villalobos FJ, Fereres E (2002) Stomatal and photosynthetic response of olive (*Olea europaea* L.) leaves to water deficits. *Plant Cell Environ* 25:395–405. <https://doi.org/10.1046/J.0016-8025.2001.00822.X>

- Nadezhkina N, Nadezhdin V, Ferreira MI, Pitacco A (2007) Variability with xylem depth in sap flow in trunks and branches of mature olive trees. *Tree Physiol* 27:105–113. <https://doi.org/10.1093/treephys/27.1.105>
- Naresh Kumar M, Murthy CS, Sessa Sai MVR (2009) On the use of standardized Precipitation Index (SPI) for drought Intensity assessment. *Met Apps* 16:381–389. <https://doi.org/10.1002/met.136>
- Oteros J, García-Mozo H, Hervás-Martínez C, Galán C (2013) Year clustering analysis for modelling olive flowering phenology. *Int J Biometeorol* 57:545–555. <https://doi.org/10.1007/s00484-012-0581-3>
- Padilla-Díaz CM, Rodríguez-Domínguez CM, Hernández-Santana V, Pérez-Martina A, Fernandes SDM, Montero A, García JM, Fernández JE (2018) Water status, gas exchange and crop performance in a super high density olive orchard under deficit irrigation scheduled from leaf turgor measurements. *Agric Water Manag* 202:241–252. <https://doi.org/10.1016/J.AGWAT.2018.01.011>
- Pataki DE, McCarthy HR, Litvak E, Pincetl S (2011) Transpiration of urban forests in the Los Angeles metropolitan area. *Ecol Appl* 21:661–677. <https://doi.org/10.1890/09-1717.1>
- Pellegrini G, Ingrao C, Camposo S, Tricase C, Contò F, Huisinck D (2016) Application of Water Footprint to olive growing systems in the Apulia region: a comparative assessment. *J Cleaner Prod* 112:2407–2418. <https://doi.org/10.1016/j.jclepro.2015.10.088>
- Peters EB, McFadden JP, Montgomery RA (2010) Biological and environmental controls on tree transpiration in a suburban landscape. *J Geoph Res* 115:G04006. <https://doi.org/10.1029/2009JG001266>
- Rana G, Katerji N (2000) Measurement and estimation of actual evapotranspiration in the field under Mediterranean climate: a review. *Eur J Agron* 13(2–3):125–153. [https://doi.org/10.1016/S1161-0301\(00\)00070-8](https://doi.org/10.1016/S1161-0301(00)00070-8)
- Rana G, Katerji N (2008) Direct and indirect methods to simulate the actual evapotranspiration of an irrigated overhead table grape vineyard under Mediterranean conditions. *Hydrol Process* 22(2):181–188. <https://doi.org/10.1002/hyp.6570>
- Rana G, Katerji N (2009) Operational model for direct determination of evapotranspiration for well watered crops in Mediterranean region. *Theor Appl Climatol* 97(3):243–253. <https://doi.org/10.1007/s00704-008-0062-0>
- Rana G, Muschitiello C, Ferrara RM (2016) Analysis of a precipitation time series at monthly scale recorded in Molifetta (South Italy) in the XVIII century (1784–1803) and comparisons with present pluviometric regime. *Ital J Agrometeorol* 3:23–30. <https://doi.org/10.19199/2016.3.2038-5625.023>
- Rana G, Palatella L, Scanlon TM, Martinelli N, Ferrara RM (2018) CO₂ and H₂O flux partitioning in a Mediterranean cropping system. *Agric for Meteorol* 260–261:118–130. <https://doi.org/10.1016/j.agrformet.2018.06.007>
- Rana G, De Lorenzi F, Mazza G, Martinelli N, Muschitiello C, Ferrara RM (2020) Tree transpiration in a multi-species Mediterranean garden. *Agric for Meteorol* 280:107767. <https://doi.org/10.1016/j.agrformet.2019.107767>
- Rana G, De Carolis G, Gaeta L, Ruggieri S, Ferrara RM (2023) Decoupling factor, aerodynamic and canopy conductances of a hedgerow olive orchard under Mediterranean climate. *Theor Appl Climatol*. <https://doi.org/10.1007/s00704-023-04475-4>
- Rosecrance RC, Krueger WH, Milliron L, Bloese J, Garcia C, Mori B (2015) Moderate regulated deficit irrigation can increase olive oil yields and decrease tree growth in super high density ‘Arbequina’ olive orchards. *Sci Hortic* 190:75–82. <https://doi.org/10.1016/j.scienta.2015.03.045>
- SAS/STAT Software (2010) Release 9.2. SAS Institute Inc., Cary
- Scanlon TM, Kustas WP (2012) Partitioning evapotranspiration using an eddy covariance-based technique: improved assessment of soil moisture and land–atmosphere exchange dynamics. *Vadose Zone J* 11:3. <https://doi.org/10.2136/vzj2012.0025>
- Searles PS, Saravia DA, Rousseaux MC (2009) Root length density and soil water distribution in drip irrigated olive orchards in Argentina under arid conditions. *Crop past Sci* 60:280–288. <https://doi.org/10.1071/CP08135>
- Sellers PJ, Randall DA, Collatz GJ, Berry JA, Field CB, Dazlich DA, Zhang C, Collelo GD, Bounoua L (1996) A revised land surface parameterization (SiB2) for atmospheric GCMs. I. Model formulation. *J Clim* 9:676–705. [https://doi.org/10.1175/1520-0442\(1996\)009%3c0676:ARLSPF%3e2.0.CO;2](https://doi.org/10.1175/1520-0442(1996)009%3c0676:ARLSPF%3e2.0.CO;2)
- Shinohara Y, Tsuruta K, Ogura A, Noto F, Komatsu H, Otsuki K, Maruyama T (2013) Azimuthal and radial variations in sap flux density and effects on stand-scale transpiration estimates in a Japanese cedar forest. *Tree Physiol* 33(5):550–558. <https://doi.org/10.1093/treephys/tpt029>
- Sofa A, Manfreda S, Fiorentino M, Dichio B, Xiloyannis C (2008) The olive tree: a paradigm for drought tolerance in Mediterranean climates. *Hydrol Earth Syst Sci* 12:293–301. <https://doi.org/10.5194/hess-12-293-2008>
- Stanghellini C, De Lorenzi F (1994) A comparison of soil- and canopy temperature-based methods for the early detection of water stress in a simulated patch of pasture. *Irrig Sci* 14:141–146. <https://doi.org/10.1007/BF00193136>
- Tognetti R, d’Andria R, Morelli G, Calandrelli D, Fragnito F (2004) Irrigation effects on daily and seasonal variations of trunk sap flow and leaf water relations in olive trees. *Plant Soil* 263:249–264. <https://doi.org/10.1023/B:PLSO.0000047738.96931.91>
- Tognetti R, d’Andria R, Lavini A, Morelli G (2006) The effect of deficit irrigation on crop yield and vegetative development of *Olea europaea* L. (cvs. Frantoio and Leccino). *Eur J Agron* 25:356–364. <https://doi.org/10.1016/j.eja.2006.07.003>
- Tognetti R, Giovannelli A, Lavini A, Morelli G, Fragnito F, d’Andria R (2009) Assessing environmental controls over conductances through the soil–plant–atmosphere continuum in an experimental olive tree plantation of southern Italy. *Agric for Meteorol* 149:1229–1243. <https://doi.org/10.1016/j.agrformet.2009.02.008>
- Vilagrosa A, Bellot J, Vallejo VR, Gil-Pelegrin E (2003) Cavitation, stomatal conductance, and leaf dieback in seedlings of two co-occurring Mediterranean shrubs during an intense drought. *J Exp Bot* 54(390):2015–2024. <https://doi.org/10.1093/jxb/erg221>
- Villalobos FJ, Orgaz F, Testi L, Fereres E (2000) Measurement and modeling of evapotranspiration of olive (*Olea europaea* L.) orchards. *Eur J Agron* 13:155–163. [https://doi.org/10.1016/S1161-0301\(00\)00071-X](https://doi.org/10.1016/S1161-0301(00)00071-X)
- Vivaldi GA, Strippoli G, Pascuzzi S, Stellacci AM, Camposo S (2015) Olive genotypes cultivated in an adult high-density orchard respond differently to canopy restraining by mechanical and manual pruning. *Sci Hortic* 192:391–399. <https://doi.org/10.1016/j.scienta.2015.06.004>
- Wiedemann A, Marañón-Jiménez S, Rebmann C, Herbst M, Cuntz M (2016) An empirical study of the wound effect on sap flux density measured with thermal dissipation probes. *Tree Physiol* 36:1471–1484. <https://doi.org/10.1093/treephys/tpw071>
- Zhang X, Yajing W, Guirong H, Fu F, Xiaoying L, Rui G, Fengxue G, Xin H, Ziguang Y, Xiuli Z, Xurong M (2019) Atmospheric humidity and genotype are key determinants of the diurnal stomatal conductance pattern. *J Agron Crop Sci* 206:1–8. <https://doi.org/10.1111/jac.12375>
- Zhou S, Liu W, Lin W (2017) The ratio of transpiration to evapotranspiration in a rainfed maize field on the Loess Plateau of China. *Water Sci Technol Water Supply* 17(1):221–227. <https://doi.org/10.2166/ws.2016.108>
- Zuñiga M, Ortega-Farías S, Poblete-Echeverría C (2014) Use of sap flow sensors to determine transpiration of a young drip-irrigated olive orchard (‘Arbequina’) under semi-arid conditions. *Acta*

Hortic 1057:405–410. <https://doi.org/10.17660/ActaHortic.2014.1057.50>

Publisher's Note Springer Nature remains neutral with regard to jurisdictional claims in published maps and institutional affiliations.

Springer Nature or its licensor (e.g. a society or other partner) holds exclusive rights to this article under a publishing agreement with the author(s) or other rightsholder(s); author self-archiving of the accepted manuscript version of this article is solely governed by the terms of such publishing agreement and applicable law.